2012

Analysis of a Monolithic, Two-Dimensional Array of Quartz Crystal Microbalances Loaded by Mass Layers With Nonuniform Thickness

Nan Liu
University of Nebraska-Lincoln, nliu1@unl.edu

J. S. Yang
University of Nebraska-Lincoln, jyang1@unl.edu

Ji Wang
Ningbo University

Analysis of a Monolithic, Two-Dimensional Array of Quartz Crystal Microbalances Loaded by Mass Layers With Nonuniform Thickness

Nan Liu, Jiashi Yang, and Ji Wang

***Abstract*—We study free thickness-shear vibrations of a monolithic, two-dimensional, and periodic array of quartz crystal microbalances loaded by mass layers with gradually varying thickness. A theoretical analysis is performed using Mindlin's two-dimensional plate equation. It is shown that the problem is mathematically governed by Mathieu's equation with a spatially varying coefficient. A periodic solution for resonant frequencies and modes is obtained and used to examine the effects of the mass layers. Results show that the vibration may be trapped or untrapped under the mass layers. The trapped modes decay differently in the two in-plane directions of the plate. The mode shapes and the decay rate of the trapped modes are sensitive to the mass layer thickness.**

I. Introduction

Quartz crystal microbalances (QCMs) are quartz crystal resonators (QCRs), operating with plate thickness-shear (TSh) modes, used for monitoring thin-film deposition and mass sensing based on the inertial effect of the mass layers on the frequencies of the QCRs. The effects of a mass layer on a QCR are multifold, including the mass density, elastic constants, and thickness. In the simplest description (the well-known Sauerbrey equation), the inertia of a mass layer lowers the frequencies of a QCR [1], [2]. This has been used to measure the product of the mass layer density and thickness. Researchers also developed more sophisticated models based on pure TSh modes, showing both the inertial and the stiffness effects [3], [4]. More references can be found in review articles such as [5] and [6].

Pure thickness-mode models for QCMs are only valid for uniform mass layers on unbounded plates, without in-plane variations or edge effects. The behavior of real devices is more complicated and can deviate from the pure thickness-mode models. For example, in a typical QCM, the mass layer covers only the central portion of the crystal plate. In this case, the TSh vibration is nonuniform; it is mainly under the mass layer and decays rapidly away from the edge of the mass layer. This phenomenon is called energy trapping [7]. It is crucial to device mounting, which can be done at the edge of a plate where there is little vibration. Thus, mounting will not affect the vibration of the plate. The in-plane variations of the TSh modes also cause deviation from the Sauerbrey equation. There have been a few attempts to consider in-plane variations of TSh modes [8]–[10]. Overall, theoretical results on this issue are few and scattered. Another situation in which the in-plane variations must be dealt with is the analysis of monolithic arrays of QCMs in which a quartz plate is loaded by patches of mass layers. In QCM arrays, the TSh vibration is large under the patches and small between them as a result of energy trapping. One-dimensional arrays of resonators [11], QCMs [12], [13], and transducers [14] were analyzed using equations for piezoelectric plates. In [11]–[14], the electrodes or mass layers on the QCRs are uniform.

It was pointed out in [15] that the mass layer on a QCM is often nonuniform and there is a lack of understanding about this. Although there have been a few results on nonuniform mass layers [16], [17] or electrodes [18]–[21] on QCRs, these analyses are all for strip resonators with the mass layer thickness variation depending on one in-plane coordinate only. In our recent papers [22], [23], a single QCM loaded by a nonuniform mass layer with a stepped [22] or a gradually varying [23] thickness was analyzed, in which the mass layer varies in both of the in-plane directions. As seen in [22], [23], nonuniform mass layers are associated with differential equations with spatially varying coefficients and are mathematically challenging. In this paper, we study the more general situation of a monolithic array of QCMs. Our analysis is different from the array analyses in [11]–[14] in two aspects. One is that the mass layers are of continuously varying thickness. The other is that we consider a two-dimensional array. A theoretical analysis is performed using Mindlin's plate equation [24], [25] for TSh vibrations of a quartz plate.

II. Governing Equations

Consider an AT-cut quartz plate, as shown in Fig. 1. It functions as a periodic array of rectangular QCMs. Only

Manuscript received November 17, 2011; accepted December 25, 2011. This work was partially supported by the U.S. Army Research Office (grant number W911NF-10-1-0293). It was also partially supported by a grant from the National Natural Science Foundation of China (grant number 10932004); the Industrial Technology Research Program of the City of Ningbo (grant number 2007B10052); and the K. C. Wong Magna Fund of Ningbo University.

N. Liu and J. Yang are with the Department of Mechanical and Materials Engineering, University of Nebraska-Lincoln, Lincoln, NE (e-mail: jyang1@unl.edu).

J. Wang is with the Piezoelectric Device Laboratory, School of Mechanical Engineering and Mechanics, Ningbo University, Ningbo, Zhejiang, China.

DOI: http://dx.doi.org/10.1109/TUFFC.2012.2252

nine of them are shown. The plate has a uniform thickness $2h$ and a mass density ρ. There is an identical thin mass layer with a slowly varying thickness on the top of each QCM. The density of the mass layer is ρ'. Its varying thickness is $2h'(x_1, x_3)$. The specific form of this function will be given later. The mass layer is assumed to be very thin. Only its inertia will be considered. Its stiffness will be neglected [1], [2]. Quartz is a material with very weak piezoelectric coupling. For a frequency analysis, we will neglect the small piezoelectric couplings as usual. In general, TSh vibration may be coupled to flexural motion. This coupling depends on the plate dimensions and is strong only for certain aspect ratios (length/thickness) of the plate [24]. For thin plates, coupling is less likely to occur. For our purpose, it is sufficient to assume that the coupling to flexure has been avoided through design. Therefore, we consider pure TSh vibration only with the following approximate displacement field [24]:

$$u_1(x_1, x_2, x_3, t) \cong x_2\psi_1(x_1, x_3, t), \quad u_2 \cong 0, \quad u_3 \cong 0, \tag{1}$$

where $\psi_1(x_1, x_3, t)$ is the plate fundamental TSh displacement. $x_2\psi_1$ has one nodal point along the plate thickness, which is at the plate's middle plane. We consider free vibration with a frequency ω, which is to be determined. The governing equation for ψ_1 is [24], [25]

$$\gamma_{11}\frac{\partial^2\psi_1}{\partial x_1^2} + \gamma_{55}\frac{\partial^2\psi_1}{\partial x_3^2} - 3h^{-2}\kappa^2 c_{66}\psi_1 + (1+3R)\rho\omega^2\psi_1 = 0, \tag{2}$$

where

$$\kappa^2 = \frac{\pi^2}{12}(1+R), \tag{3a}$$

$$R = \frac{\rho' h'}{\rho h}, \tag{3b}$$

$$\gamma_{11} = \frac{s_{33}}{s_{11}s_{33} - s_{13}^2}, \quad \gamma_{55} = \frac{1}{s_{55}}. \tag{4}$$

s_{pq} are the usual elastic compliances. Eq. (2) can be written as

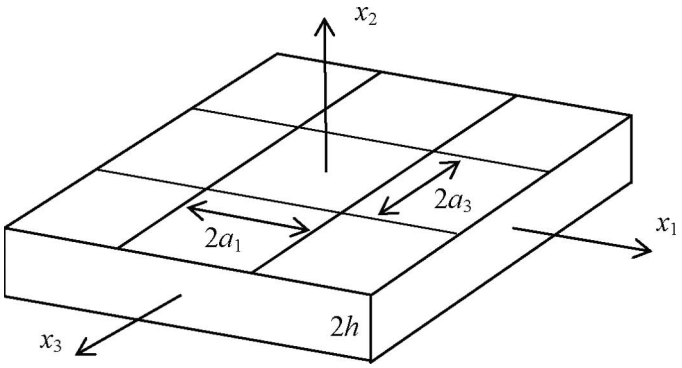

Fig. 1. Coordinate system for a quartz plate with a 3 × 3 array of quartz crystal microbalances.

$$\gamma_{11}\frac{\partial^2\psi_1}{\partial x_1^2} + \gamma_{55}\frac{\partial^2\psi_1}{\partial x_3^2} - \rho\omega_\infty^2(1+R)\psi_1 + (1+3R)\rho\omega^2\psi_1 = 0, \tag{5}$$

where we have denoted

$$\omega_\infty = \frac{\pi}{2h}\sqrt{\frac{c_{66}}{\rho}}, \tag{6}$$

which is the frequency of the fundamental TSh mode of the crystal plate when the mass layers are not present. Rearranging terms, we can further write (5) as

$$\gamma_{11}\frac{\partial^2\psi_1}{\partial x_1^2} + \gamma_{55}\frac{\partial^2\psi_1}{\partial x_3^2} + \rho(\omega^2 - \omega_\infty^2)\psi_1 + 2R\rho\omega^2\psi_1 = 0. \tag{7}$$

Because R is very small, the last term of the left-hand side of (7) is also very small. Therefore, in this term, we make the approximation that $\omega^2 \cong \omega_\infty^2$. The error is of the order of $R(\omega^2 - \omega_\infty^2)$, a high-order small quantity because $\omega^2 - \omega_\infty^2$ is also small. Under this approximation, (7) becomes

$$\gamma_{11}\frac{\partial^2\psi_1}{\partial x_1^2} + \gamma_{55}\frac{\partial^2\psi_1}{\partial x_3^2} + [\rho\omega^2 - \rho\omega_\infty^2(1-2R)]\psi_1 = 0. \tag{8}$$

We consider the case when the varying mass layer thickness can be written as

$$2h' = 2h_0[1 - f_1(x_1) - f_3(x_3)], \tag{9}$$

where $2h_0$ is the mass layer center thickness, and f_1 and f_3 are small and slowly growing functions so that the mass layer is thick at the center and thin at its edges. Corresponding to (9), from (3b) we have

$$R = R_0[1 - f_1(x_1) - f_3(x_3)], \tag{10}$$

where

$$R_0 = \frac{\rho' h_0}{\rho h}. \tag{11}$$

Substitution of (10) into (8) gives

$$\gamma_{11}\frac{\partial^2\psi_1}{\partial x_1^2} + \gamma_{55}\frac{\partial^2\psi_1}{\partial x_3^2} + [\rho\omega^2 - \rho\omega_0^2 - \rho\omega_\infty^2 2R_0(f_1+f_3)]\psi_1 = 0, \tag{12}$$

where we have denoted

$$\omega_0^2 = \omega_\infty^2(1-2R_0). \tag{13}$$

ω_0 is the frequency of the fundamental TSh mode of the crystal plate with a mass layer of a uniform thickness $2h_0$. We are mainly interested in the so-called energy-trapped modes with the frequency ω within

$$\rho\omega_1^2 A_0 + \frac{1}{4}\rho\omega_\infty^2 R_0 A_1 + \left\{\frac{1}{2}\rho\omega_\infty^2 R_0 A_0 + \left[\rho\omega_1^2 - \gamma_{11}\left(\frac{\pi}{a_1}\right)^2\right]A_1 + \frac{1}{4}\rho\omega_\infty^2 R_0 A_2\right\}\cos\frac{\pi x_1}{a_1}$$
$$+ \sum_{n=2}^{\infty}\left\{\frac{1}{4}\rho\omega_\infty^2 R_0 A_{n-1} + \left[\rho\omega_1^2 - \gamma_{11}\left(\frac{n\pi}{a_1}\right)^2\right]A_n + \frac{1}{4}\rho\omega_\infty^2 R_0 A_{n+1}\right\}\cos\frac{n\pi}{a_1}x_1 = 0. \tag{24}$$

$$\omega_0 < \omega < \omega_\infty. \tag{14}$$

III. Free Vibration Analysis

As a partial differential equation, (12) is separable. Let

$$\psi_1(x_1, x_3) = F_1(x_1)F_3(x_3). \tag{15}$$

Then, from (12), by the standard procedure of separation of variables, we obtain

$$\begin{aligned}\gamma_{11}F_{1,11} + \rho\bar{\omega}_1^2 F_1 - \rho\omega_\infty^2 2R_0 f_1(x_1)F_1 = 0,\\ \gamma_{55}F_{3,33} + \rho\bar{\omega}_3^2 F_3 - \rho\omega_\infty^2 2R_0 f_3(x_3)F_3 = 0,\end{aligned} \tag{16}$$

where the separation constants $\bar{\omega}_1$ and $\bar{\omega}_3$ must satisfy the following equation, which gives the resonant frequencies once $\bar{\omega}_1$ and $\bar{\omega}_3$ are determined:

$$\omega^2 = \omega_0^2 + \bar{\omega}_1^2 + \bar{\omega}_3^2. \tag{17}$$

To describe a mass layer with a periodically varying thickness, and thus representing an array, we choose

$$\begin{aligned}2h' &= \frac{h_0}{2}\left(\cos\frac{\pi x_1}{a_1} + \cos\frac{\pi x_3}{a_3}\right) + h_0\\ &= 2h_0\left[1 - \left(\frac{1}{4} - \frac{1}{4}\cos\frac{\pi x_1}{a_1}\right) - \left(\frac{1}{4} - \frac{1}{4}\cos\frac{\pi x_3}{a_3}\right)\right],\end{aligned} \tag{18}$$

where a_1 and a_3 are the length and the width of an individual QCM, respectively. In a typical QCM, e.g., the one at the origin with $|x_1| < a_1$ and $|x_3| < a_3$, the mass layer described by (18) assumes its maximal thickness $2h_0$ at the center $(0,0)$ and it vanishes at the four corners of the rectangle. Therefore, (18) describes a mass layer thick at the center and thin at the edges. In other QCMs of the array, we have the same nonuniform mass layer because of the periodicity of (18). From (18) and (9), we identify

$$f_1 = \frac{1}{4} - \frac{1}{4}\cos\frac{\pi x_1}{a_1}, \quad f_3 = \frac{1}{4} - \frac{1}{4}\cos\frac{\pi x_3}{a_3}. \tag{19}$$

Then, (16) can be written as

$$\gamma_{11}F_{1,11} + \left(\rho\omega_1^2 + \frac{1}{2}\rho\omega_\infty^2 R_0\cos\frac{\pi x_1}{a_1}\right)F_1 = 0, \tag{20}$$

$$\gamma_{55}F_{3,33} + \left(\rho\omega_3^2 + \frac{1}{2}\rho\omega_\infty^2 R_0\cos\frac{\pi x_3}{a_3}\right)F_3 = 0, \tag{21}$$

where, for convenience, we have introduced ω_1 and ω_3, which satisfy the following equation from (17):

$$\omega^2 = \omega_0^2 + \omega_1^2 + \omega_3^2 + \omega_\infty^2 R_0. \tag{22}$$

Eqs. (20) and (21) are the well-known Mathieu's equation [26]. For the periodic array in Fig. 1, we are interested in periodic solutions of (20) and (21) that are even functions of x_1 and x_3. Therefore, according to Fourier series, we let

$$F_1 = A_0 + \sum_{n=1}^{\infty} A_n\cos\frac{n\pi}{a_1}x_1, \tag{23a}$$

$$F_3 = B_0 + \sum_{n=1}^{\infty} B_n\cos\frac{n\pi}{a_3}x_3, \tag{23b}$$

where A_n $(n = 0, 1, 2, \ldots)$ are undetermined coefficients. Eqs. (20) and (21) can be solved in the same way. We focus on (20) in the following. Substituting (23a) into (20) and using the relevant trigonometric identity to convert the product terms into sums, we obtain (24), see above. Multiplying both sides of (24) by $\cos(m\pi x_1/a_1)$ with $m = 0, 1, 2, \ldots$, integrating the resulting expression over a period $(-a_1, a_1)$, and using the orthogonality of the trigonometric functions, we arrive at the following recurrence relations, which are linear homogeneous equations for A_m:

$$\begin{aligned}&\rho\omega_1^2 A_0 + \frac{1}{4}\rho\omega_\infty^2 R_0 A_1 = 0,\\ &\frac{1}{2}\rho\omega_\infty^2 R_0 A_0 + \left[\rho\omega_1^2 - \gamma_{11}\left(\frac{\pi}{a_1}\right)^2\right]A_1 + \frac{1}{4}\rho\omega_\infty^2 R_0 A_2 = 0,\\ &\frac{1}{4}\rho\omega_\infty^2 R_0 A_{m-1} + \left[\rho\omega_1^2 - \gamma_{11}\left(\frac{m\pi}{a_1}\right)^2\right]A_m\\ &\qquad + \frac{1}{4}\rho\omega_\infty^2 R_0 A_{m+1} = 0, \qquad m = 2, 3, 4, \ldots.\end{aligned} \tag{25}$$

For nontrivial solutions of A_m, the determinant of the coefficient matrix of (25) must vanish, which gives the frequency equation that determines ω_1. The corresponding nontrivial A_m obtained from (25) determines F_1 through (23a). In a similar way, ω_3 and B_m can be obtained by solving (21). Then, ω can be obtained from (22). These will be done numerically on a computer.

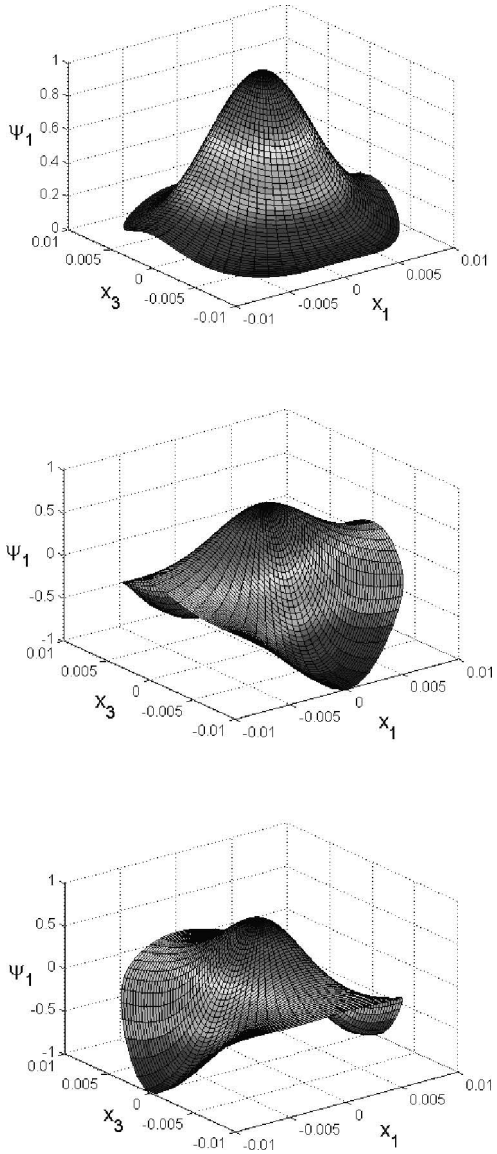

Fig. 2. The three modes found within $\omega_0 < \omega < \omega_\infty$ (shown in a single quartz crystal microbalance).

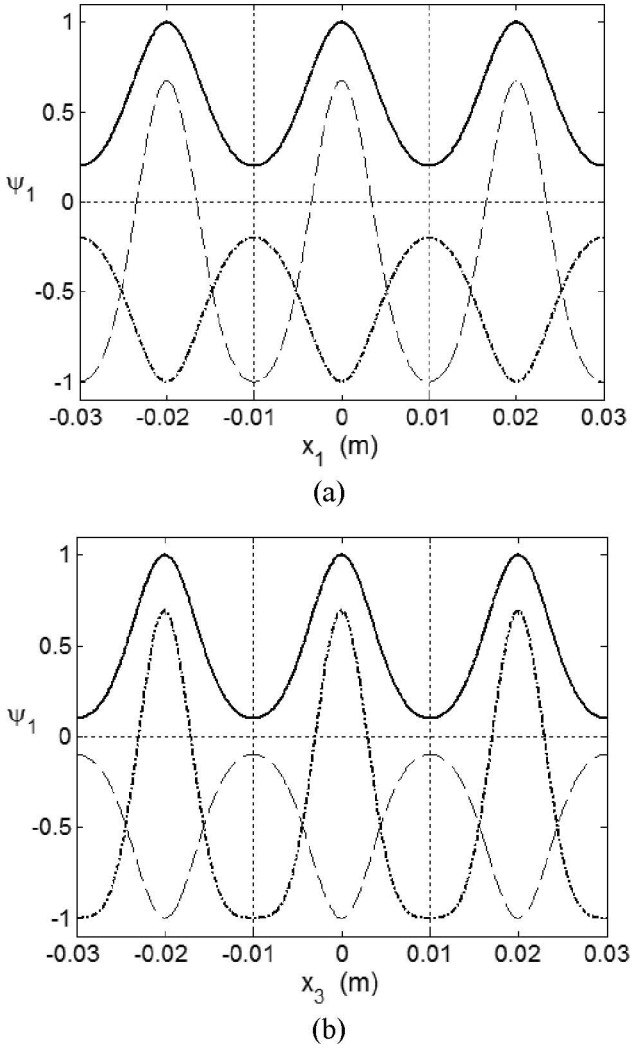

Fig. 3. (a) x_1 dependence and (b) x_3 dependence of the three modes in a 3×3 array: solid line: the first mode; dash-dotted line: the second mode; dashed line: the third mode.

IV. Numerical Results

For numerical examples, we fix $2h = 1$ mm and $a_1 = a_3 = 1$ cm, which are typical dimensions for a QCM. We consider the case of $R_0 = 5\%$. In this case, $f_\infty = 1\,654\,638$ Hz and $f_0 = 1\,569\,727$ Hz. Table I shows the results of numerical tests using three, five, or ten terms in the Fourier series. Three resonant frequencies, f_{11}, f_{12}, and f_{21}, are found within $\omega_0 < \omega < \omega_\infty$. It can be seen that the frequencies are already indistinguishable when using five and ten terms. Numerical tests also show that when using ten terms in the series, the modes corresponding to the three frequencies also become stable. This is expected because, as will be seen later, the behaviors of the modes we are interested in are relatively simple, with only a few in-plane oscillations, and therefore can be well approximated by a few terms in the Fourier series. Our subsequent calculations will be based on ten terms in the series.

TABLE I. Resonant Frequencies Showing Convergence.

Number of terms in the Fourier series	f_{11} (Hz)	f_{12} (Hz)	f_{21} (Hz)
3	1 595 188	1 626 922	1 631 909
5	1 595 181	1 626 864	1 631 890
10	1 595 181	1 626 864	1 631 890

For the three modes found, Fig. 2 shows their vibration distribution in a single QCM, e.g., the one within $|x_1| < a_1$ and $|x_3| < a_3$. The first mode is at the frequency f_{11}, the lowest frequency. The vibration is large near the center and decays to almost zero near the edges. Therefore, this is a well-trapped mode. For this mode, neighboring QCMs have little interaction, which is the desired situation for a QCM array. The second mode is at f_{12}. It is well trapped along x_1 and is nearly zero at $x_1 = \pm a_1$. However, it changes its sign along x_3 with two nodal points and has a large amplitude near $x_3 = \pm a_3$. Therefore, for this mode, in the x_3 direction, the vibration leaks out of the mass layer and neighboring QCMs begin to interact significantly.

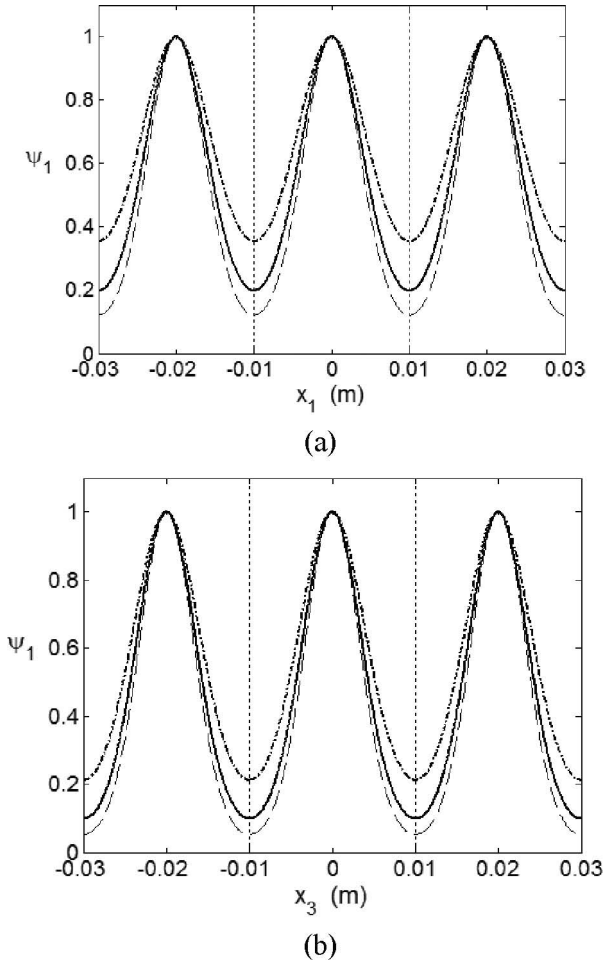

Fig. 4. Effects of R_0 on vibration distribution of the first mode along (a) x_1 and (b) x_3 in a 3 × 3 array: dash-dotted line: $R_0 = 3\%$; solid line: $R_0 = 5\%$; dashed line: $R_0 = 7\%$.

Similarly, the third mode at f_{21} is well trapped along x_3 but has two nodal points along x_1 and a large amplitude near $x_1 = \pm a_1$.

To see the variations of the three modes found more clearly, in Fig. 3 we plot their x_1 dependence and x_3 dependence separately for a 3 × 3 array of QCMs. Clearly, the first mode is trapped in both directions, the second mode is trapped in the x_1 direction only, and the third mode is trapped in the x_3 direction only. We note that the modes decay faster in the x_3 direction than in the x_1 direction. Therefore, rectangular QCMs with $a_3 < a_1$ are more reasonable than square QCMs for device miniaturization. Similarly, elliptical QCMs are more reasonable than circular ones. Fig. 3 also shows that even for the first mode there is still some vibration left between neighboring QCMs.

Fig. 4 shows the effect of the mass ratio R_0 on the vibration distribution of the first mode for a 3 × 3 array of QCMs. A larger R_0 represents a mass layer that is thicker at the center. The figure shows that a thicker mass layer is associated with fast decay of the vibration amplitude from the center and smaller vibration amplitude between neighboring QCMs or less interaction among them.

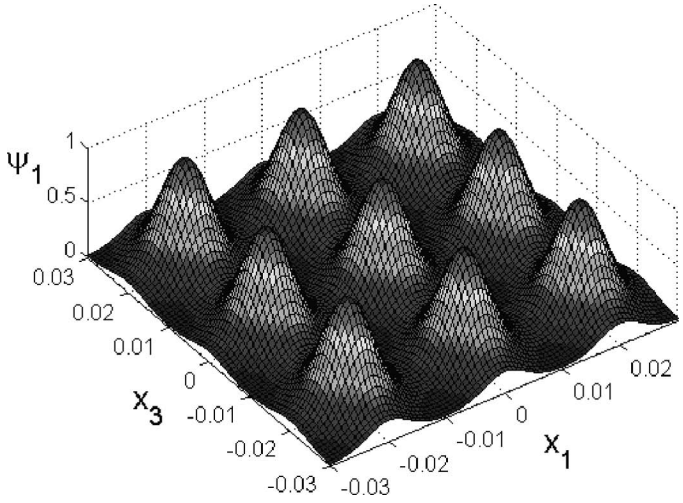

Fig. 5. Vibration distribution of the first mode in a 3 × 3 array.

For a more visual presentation, in Fig. 5 we show the vibration distribution of the first mode in a 3 × 3 array of QCMs.

V. Conclusion

Using Mindlin's equation for a quartz plate, a periodic array of QCMs with nonuniform mass layers is governed by Mathieu's equation with a spatially varying periodic coefficient whose periodic solution can be obtained by Fourier series. Numerical results show that there exist both trapped and untrapped modes. The trapped modes decay differently along x_1 and x_3. Therefore, rectangular and elliptical QCMs are better designs than square and circular ones. The trapped modes decay faster for mass layers that are thicker at the center.

References

[1] A. Ballato and T. J. Lukaszek, "Mass-loading of thickness-excited crystal resonators having arbitrary piezo-coupling," *IEEE Trans. Sonics Ultrason.*, vol. 21, no. 4, pp. 269–274, 1974.

[2] J. A. Kosinski, "Thickness vibration of flat piezoelectric plates with massy electrodes of unequal thickness," in *Proc. IEEE Ultrasonics Symp.*, 2003, pp. 70–73.

[3] J. G. Miller and D. J. Bolef, "Acoustic wave analysis of the operation of quartz-crystal film-thickness monitors," *J. Appl. Phys.*, vol. 39, no. 12, pp. 5815–5816, 1968.

[4] F. Boersma and E. C. van Ballegooyen, "Rotated Y-cut quartz crystal with two different electrodes treated as a one-dimensional acoustic composite resonator," *J. Acoust. Soc. Am.*, vol. 62, no. 2, pp. 335–340, 1977.

[5] E. Benes, M. Gröschl, W. Burger, and M. Schmid, "Sensors based on piezoelectric resonators," *Sens. Actuators A Phys.*, vol. 48, no. 1, pp. 1–21, 1995.

[6] E. P. EerNisse "Quartz resonators vs their environment: Time base or sensor?" *Jpn. J. Appl. Phys.*, vol. 40, no. 5B, pp. 3479–3483, 2001.

[7] D. Salt, *Hy-Q Handbook of Quartz Crystal Devices.* Wokingham, UK: Van Nostrand Reinhold, 1987.

[8] P. J. Cumpson and M. P. Seah, "The quartz crystal microbalances; Radial/polar dependence of mass sensitivity both on and off the electrodes," *Meas. Sci. Technol.*, vol. 1, no. 7, pp. 544–555, 1990.

[9] F. Josse and Y. Lee, "Analysis of the radial dependence of mass sensitivity of modified electrode quartz crystal resonators," *Anal. Chem.*, vol. 70, no. 2, pp. 237–247, 1998.

[10] B. A. Martin and H. E. Hager, "Velocity profile on quartz crystals oscillating in liquids," *J. Appl. Phys.*, vol. 65, no. 7, pp. 2630–2635, 1989.
[11] W. D. Beaver, "Analysis of elastically coupled piezoelectric resonators," *J. Acoust. Soc. Am.*, vol. 43, no. 5, pp. 972–981, 1968.
[12] F. Shen, K. H. Lee, S. J. O'Shea, P. Lu, and T. Y. Ng, "Frequency interference between two quartz crystal microbalances," *IEEE Sens. J.*, vol. 3, no. 3, pp. 274–281, 2003.
[13] F. Shen and P. Lu, "Influence of interchannel spacing on the dynamical properties of multichannel quartz crystal microbalance," *IEEE Trans. Ultrason. Ferroelectr. Freq. Control*, vol. 51, no. 2, pp. 249–253, 2004.
[14] H. Li, H. L. Du, L. M. Xu, Y. T. Hu, H. Fan, and J. S. Yang, "Analysis of multilayered thin-film piezoelectric transducer arrays," *IEEE Trans. Ultrason. Ferroelectr. Freq. Control*, vol. 56, no. 11, pp. 2571–2577, 2009.
[15] J. R. Vig and A. Ballato, "Comments about the effects of nonuniform mass loading on a quartz crystal microbalance," *IEEE Trans. Ultrason. Ferroelectr. Freq. Control*, vol. 45, no. 5, pp. 1123–1124, 1998.
[16] C. van der Steen, F. Boersma, and E. C. van Ballegooyen, "The influence of mass loading outside the electrode area on the resonant frequencies of a quartz-crystal microbalance," *J. Appl. Phys.*, vol. 48, no. 8, pp. 3201–3205, 1977.
[17] E. C. van Ballegooyen, F. Boersma, and C. van der Steen, "Influence of the thickness of tabs on the resonating properties of a quartz crystal," *J. Acoust. Soc. Am.*, vol. 62, no. 5, pp. 1189–1195, 1977.
[18] J. S. Yang, H. Xue, H. Y. Fang, Y. T. Hu, J. Wang, and L. J. Shen, "Effects of electrodes with varying thickness on energy trapping in thickness-shear quartz resonators," *IEEE Trans. Ultrason. Ferroelectr. Freq. Control*, vol. 54, no. 4, pp. 892–895, 2007.
[19] J. Wang, L. J. Shen, and J. S. Yang, "Effects of electrodes with continuously varying thickness on energy trapping in thickness-shear mode quartz resonators," *Ultrasonics*, vol. 48, no. 2, pp. 150–154, 2008.
[20] J. S. Yang, Z. G. Chen, and H. P. Hu, "Electrically forced vibration of a thickness-twist mode piezoelectric resonator with non-uniform electrodes," *Acta Mech. Solida Sin.*, vol. 20, no. 3, pp. 266–274, 2007.
[21] J. S. Yang, Z. G. Chen, and Y. T. Hu, "Vibration of a thickness-twist mode piezoelectric resonator with asymmetric, non-uniform electrodes," *IEEE Trans. Ultrason. Ferroelectr. Freq. Control*, vol. 55, no. 4, pp. 841–848, 2008.
[22] N. Liu, J. S. Yang, and W. Q. Chen, "Effects of mass layer nonuniformity on a quartz crystal microbalance," *IEEE Sens. J.*, vol. 11, no. 4, pp. 934–938, 2011.
[23] N. Liu, J. S. Yang, and W. Q. Chen, "Effects of a mass layer with gradually varying thickness on a quartz crystal resonator," *IEEE Sens. J.*, vol. 11, no. 8, pp. 1635–1639, 2011.
[24] R. D. Mindlin, "Thickness-shear and flexural vibrations of crystal plates," *J. Appl. Phys.*, vol. 22, no. 3, pp. 316–323, 1951.
[25] R. D. Mindlin and P. C. Y. Lee, "Thickness-shear and flexural vibrations of partially plated, crystal plates," *Int. J. Solids Struct.*, vol. 2, no. 1, pp. 125–139, 1966.
[26] A. H. Nayfeh, *Introduction to Perturbation Techniques*. New York, NY: Wiley, 1981.

Authors' photographs and biographies were unavailable at time of publication.